Art. N° 376
Contribution COB N° 528

Reprinted from Melson, W. G., Rabinowitz, P. D., et al., 1978.
Initial Reports of the Deep Sea Drilling Project, Volume XLV, Washington (U.S. Government Printing Office)

22. TRACE ELEMENTS IN BASALTS FROM 23°N and 36°N IN THE ATLANTIC OCEAN: FRACTIONAL CRYSTALLIZATION, PARTIAL MELTING, AND HETEROGENEITY OF THE UPPER MANTLE[1]

H. Bougault, Centre Océanoligique de Bretagne, Brest, France
M. Treuil, Laboratoire P. Sue, Saclay, France
and
J.L. Joron, Institut de Physique du Globe, Universite Paris VI, Paris, France

INTRODUCTION

From a study of first-transition series trace elements and low-partition-coefficient trace elements or so-called hygromagmatophyle elements (Treuil and Varet, 1973; Treuil and Joron, 1976), we will try to define the relative importance of the three fundamental parameters—mantle source composition, extent of partial melting, and crystal fractionation—which bear on the formation of basalts recovered during Leg 45. We relate the presented data to the results of shipboard study (Chapters 7 and 8, this volume) and then give a tentative interpretation, taking into account our present knowledge of the behavior of trace elements during magmatic processes of FAMOUS and Leg 37 results.

LEG 45 SAMPLES; DESCRIPTION OF RESULTS

Both major element and trace element data are presented in this section. The major oxides SiO_2, Al_2O_3, Fe_2O_3 total, MgO, CaO, K_2O, TiO_2, and the trace elements Sr, Zr, Ni, and Cr were analyzed on-board ship, in collaboration with J. M. Rhodes (see Introduction and Site Chapters, this volume). Analyses for MnO, P_2O_5, and Na_2O were completed on shore. FeO determinations were made by J. Norberg (Smithsonian Institution) according to the method outlined by L. C. Peck (1964).

All major element data presented were determined by X-ray fluorescence, except Na_2O, which was determined by atomic absorption. Trace element data were obtained by X-ray fluorescence (XRF), neutron activation (NA), or atomic absorption (AA). Co, Ni, and Zr were analyzed by both X-ray fluorescence and neutron activation; both results are given.

Trace element XRF determinations were corrected for matrix and instrumental effects by the procedures of Bougault et al. (1977); in addition, V and Cr measurements were corrected for the effects of enhancement and overlapping lines (Ti Kβ and V Kβ, respectively.

The shipboard values for Cr are only approximate, because it was not possible on board to calculate the full matrix correction including the effect of iron enhancement and V Kβ interference.

The neutron activation method used was pure instrumental activation analysis (without chemical separation), using epithermal neutron irradiation (OSIRIS Reactor in Saclay—C.E.A. Groupe Pierre Suë). Because of the low order of magnitude of the concentrations of investigated elements in tholeiites (Tb, Hf, Ta. . .), the use of epithermal neutrons is very important; this kind of irradiation allows the interaction of ^{46}Sc and ^{55}Fe to be strongly diminished. Irradiation was performed under Cd vials; then several measurements were made using a Ge-Li detector (resolution 2 KeV at 1.33 MeV) at different times from four days to one month after irradiation. The reference standards used are GSN and BCR1.

Tables 1 and 2 for Hole 395, Tables 3 and 4 for Hole 395A, and Tables 5 and 6 for Hole 396 show the concentrations of elements (major elements expressed in per cent and trace elements in ppm) for the samples investigated on-board ship.

Several different chemical units were defined on board (see Chapters 7 and 8, this volume), as shown by Figure 1, where concentrations of selected major and trace elements are plotted against depth. Units A_2 through A_5 are aphyric units, and P_2 through P_5 are porphyritic units. Some units were hard to define, because only one sample representing them was analyzed, or a given sample chemically seemed outside the range of analyses characterizing the unit. This is the case for Sample 395A-11-1, 105-107 cm; even though major elements resolve little difference between this sample and Unit A_2*, additional trace element data appear to suggest a real difference between them. In Hole 395A, phyric units are named P_2 to P_5, as a function of depth; In Hole 395, Samples 18-1, 37-41 cm and 18-2, 33-38 cm (Unit P_1*) are chemically similar to Unit P3 of Hole 395A.

Sample 395-20-1, 32-36 cm, within Unit P_2*, nevertheless does not belong to that unit; it stands alone. Sample 395A-15-5, 0-11 cm, situated at the boundary of Units P_2 and P_3, remains difficult to classify; it is chemically similar to Unit P_5. The average composition given in Table 7 for Unit P_5 does not take into account breccia samples (which differ mainly in Cr and Ni). The deepest aphyric sample, 395A-67-2, 54-59 cm, is classified as belonging to Unit A_4; in fact, it is very similar to samples of Unit A_3.

[1]Contribution 528 of the Département Scientifique, Centre Océanologique de Bretagne.

TABLE 1
Site 395, Hole 395, Major-Element Data (volatile-free concentrations, wt. %)

Unit				A2*			A2*					P1*		P1*		A2*	P2*
Sample (Interval in cm)	10, CC (#1)	10, CC (#2)	10, CC (#3)	11-1, 105-107	11-2, 62-64	12-2, 109-111	14-1, 112-114	14-1, 131-132	15-1, 71-73	15-1, 112-115	15-2, 130-133	17-1, 56-59	18-1, 37-41	18-1, 61-70	18-2, 33-38	18-2, 85-95	19-1, 18-20	20-1, 32-36
Depth (m)	93	93	93	101	102	112	131	131	139	139	140	159	166	167	168	169	177	185
Rock Type	s	G	s	VB	aphy. B	aphy. B	al B	aphy. B	aphy. B	aphy. B	aphy. B	G	pl. Pyr B	s	pl. pyr. B	s	aphy. B	pl. B
SiO_2	43.6	45.7	44.8	48.9	49.3	49.8	47.01	49.7	49.81	49.1	49.0	50.2	49.4	43.1	49.4	43.4	49.8	49.6
Al_2O_3	1.26	24.24	6.27	15.93	14.88	15.11	16.79	14.94	15.11	15.01	14.75	17.71	17.32	0.91	18.21	1.37	15.08	18.77
Fe_2O_3 (t)	9.95	3.81	10.66	12.83	11.95	11.90	13.76	11.97	11.76	12.05	12.22	6.52	8.62	10.25	8.37	9.36	11.05	9.52
FeO	0.93		4.35	6.96		8.10		7.53				4.62	5.67	4.55		3.10	7.41	4.47
MnO	0.13	0.07	0.10	0.20	0.18	0.18	0.20	0.17	0.17	0.17	0.18	0.11	0.14	0.11	0.14	0.10	0.19	0.14
MgO	43.7	13.9	35.3	6.8	8.5	8.9	6.64	8.3	7.47	8.6	8.5	12.2	8.5	44.3	7.9	42.0	8.5	6.1
CaO	0.03	12.61	1.85	11.01	10.49	10.50	10.93	10.56	10.92	10.53	10.54	9.32	12.58	0.89	12.85	2.09	11.25	12.05
Na_2O	0.00	1.15	0.00	2.88	2.83	2.85	2.90	2.88	2.85	2.88	2.85	3.53	2.38	0.03	2.33	0.00	2.75	2.79
K_2O	0.02	0.08	0.02	0.22	0.09	0.09	0.28	0.13	0.25	0.10	0.13	0.20	0.07	0.00	0.13	0.00	0.31	0.30
TiO_2	0.03	0.04	0.09	1.70	1.61	1.61	1.83	1.63	1.61	1.62	1.62	0.39	1.01	0.03	1.02	0.04	1.65	1.28
P_2O_5	0.01	0.02	0.02	0.18	0.15	0.13	0.22	0.15	0.14	0.15	0.15	0.02	0.10	0.02	0.12	0.00	0.16	0.13
Total	98.73	101.62	99.11	100.65	99.98	101.07	100.36	100.43	100.09	100.21	99.94	100.20	100.12	99.64	100.47	98.36	100.84	100.68
LoI	-13.8	-4.2	-11.6	-0.9	-1.1	-1.3	-8.7	-1.2	-9.5	-1.5	-0.8	-4.9	-1.4	-7.6	-0.6	-9.1	-1.0	-1.5

Note: G = gabbro, s = serpentinite, V = variolitic, B = basalt, aphy. = aphyric, pl = plagioclase, al = altered.

In Hole 396, three units have been recognized, named P_a, P_b, and P_c, as a function of depth and are listed in Tables 5 and 6.

All the trace element results obtained confirm the classification and the definitions of chemical units made on-board ship. Since we bring no change or very little change to the definition of chemical units, we ask the reader to examine Chapters 7 and 8 in this volume for detailed information about particular units.

The alkali metals, Cs and Rb, together with Sr, show variations even within a given unit. Average values of other elements, which are more homogeneous within a given unit, are reported for each unit, together with associated σ (standard deviation) values, in Tables 7, 8, 9, and 10 for Sites 395 and 396, respectively. Examination of Tables 7 and 10 shows that concentrations of all elements investigated are typical of mid-ocean ridge tholeiites. Nevertheless, Th and Ta values are rather low, and some Sr values are high, especially in phyric units P_2* of Hole 395, P_2 and P_5 of Hole 395A. This problem of high Sr is still being investigated to determine if what we are seeing is enriched Sr because of plagioclase phenocrysts or is a result of alteration effects (since many vesicles filled with secondary minerals are present in these samples). Generally, trace element concentrations, except for Ni and Cr, are lower within phyric units than in aphyric units; this can be explained in part by the dilution effect of phenocrysts (mainly plagioclase), since many of these elements have low partition coefficients and low abundances in phenocryst phases, especially plagioclase.

Sc and Co vary within a narrow range, 30 to 38 ppm and 38 to 48 ppm, respectively, and show only a slight difference between aphyric and phyric units, as mentioned above. Taking into account the dilution effect of phenocrysts, one would obtain roughly similar concentrations for the matrix of phyric units as for aphyric units. Finding so little variation for those elements means that their behavior depends little on crystallization and melting processes; in addition, this means that the initial material (before melting) was homogeneous with respect to them. If the source had been heterogeneous, then melting and crystallization would have had to occur in such a way as to compensate for the possible variations in the initial material, and this would be purely matter of chance.

Average values of Ni and Cr for Holes 395 and 395A are reported in Table 7, except for Units P_4 and P_4 '; Ni and Cr are more variable in these units, because of a variable content of olivine and clinopyroxene phenocrysts.

ALTERATION EFFECTS

Among the trace elements investigated, three can vary considerably because of alteration: Cs, Rb, and Sr (Hart, 1971). The problem of whether strontium is enriched in plagioclase or in the matrix, or is high because of alteration, is being investigated, as already mentioned.

As Figure 1 shows, the abundance of K_2O is somewhat random even within a given unit. Similar observations can be made for Cs and Rb. Cs is plotted versus K_2O in Figure 2, and versus Rb in Figure 3. Considering all points on Figure 2, no correlation between Cs and K_2O is evident. But within each unit, a positive correlation exists between Cs and K_2O, even taking into account the analytical precision (about 0.02 ppm for Cs and 0.2% for K_2O). Cs increases linearly with K_2O from low concentrations which could be considered as initial values before secondary alteration processes. In Figure 2 a general positive correlation between Rb and Cs can be observed, but there is no possibility of distinguishing between units, because of the analytical precision in determining Rb ($\sim$1 ppm).

The general correlation Cs = f (Rb) and the intra-unit correlation of Cs = f (K_2O) contrast with the homogeneity of other trace elements within units, allowing us to state that *these variations result from secondary processes (probably alteration).*

GEOCHEMICAL METHOD OF INVESTIGATION

Properties of Trace Elements

It is assumed that trace element behavior follows the high-dilution law; as a consequence, a partition coef-

ficient between different phases can be defined directly in connection with the chemical potential of a given element in the different phases concerned. As a convention, the partition coefficient D of an element is defined as the ratio of its concentration in a mineral to its concentration in the liquid.

Among the investigated elements, one can find high-partition-coefficient (HPC) elements such as Cr and Ni ($D>1$) and low-partition-coefficient (LPC) elements such as Th and Ta ($D<<1$). The bulk partition coefficients of some elements are variable, depending on the proportion of phases in equilibrium, and in this respect, their concentrations depend on the nature of magmatic processes, such as partial melting or fractional crystallization. This is the case, for instance, for V, Co, and Sr. The diverse partition coefficients are interpreted to reflect high stabilization energy in octahedral coordination for such elements as Cr and Ni (Burns, 1970; Curtis, 1964; Orgel, 1964; Allegre et al., 1968; Bougault and Hébinian, 1974, and the ability of other elements—Ta and Th, for instance—to form stable complexes in the liquid phase (Treuil and Varet, 1973; Treuil and Joron, 1975).

Behavior of Trace Elements During Crystallization and Melting Processes

As crystallization proceeds in a given magma, we assume that that Rayleigh law is valid:

$$\frac{C_L}{C_{LO}} = F^{(D-1)}$$

where

C_L = concentration of the element in the liquid,
C_{LO} = initial concentration of the element in the liquid,
F = fraction of remaining liquid,
D = bulk partition coefficient of the element.

Considering two elements (subscripts 1 and 2), the relationship between elements 1 and 2 is:

$$\log C_{L2} = \frac{D_2-1}{D_1-1} \log C_{L_1} \qquad \text{(Eq. 1)}$$

$$+ \frac{(D_1-1)\log C_{LO2} - (D_2-1)\log C_{LO1}}{D_1 - 1}$$

1) If elements 2 and 1 have low partition coefficients, Equation 1 is simplified to:

$$C_{L2} = A\, C_{L1} \qquad A = \frac{C_{LO1}}{C_{LO2}} \qquad \text{(Eq. 2)}$$

The slope A depends on the initial concentrations in the liquid C_{LO1} and C_{LO2} (Treuil and Varet, 1973; Treuil and Joron, 1975).

2) If elements 2 and 1 have high partition coefficients and if the proportion of phases crystallizing is constant, the plot of log C_{L2} as a function of log C_{L1} is a straight line, the slope of which is

$$\frac{D_2-1}{D_1-1}$$

3) If element 2 is a HPC element and element 1 a LPC element, the slope of the line log C_{L2} = f (log C_{L1} is approximated to (D_2-1); this can be considered as a way of determining the bulk partition coefficient D_2 of element 2.

In fact, these assumptions are valid insofar as we start from given values of C_{LO2} and C_{LO1}, which means starting from a given liquid with magmatic differentiation resulting only from crystallization processes. C_{LO2} and C_{LO1} depend on partial melting; it is necessary to determine to what extent they can vary (if at all) when partial melting occurs, using the elements investigated.

When partial melting occurs, let us assume that C_{LO} is given by the formula of Shaw (1970):

$$\frac{C_{LO}}{C_{SO}} = \frac{1}{D_O + F(1-D)}$$

where

C_{LO} = concentration of the element in the liquid (which is the initial value with respect to the crystallization process),
C_{SO} = initial concentration in the solid,
D_O = initial bulk partition coefficient,
D = bulk partition coefficient corresponding to melting phases,
F = fraction of liquid produced.

Considering very low-partition-coefficient elements 1 and 2, it is easy to see that

$$\frac{C_{LO1}}{C_{LO2}} \cong \frac{C_{SO1}}{C_{SO2}}, \text{ almost independent of F.}$$

In this case, the slope A mentioned in Equation 2 is not dependent on F, and gives direct information about the initial solid (before melting) (Treuil and Joron, 1976),

$$A = \frac{C_{LO1}}{C_{LO2}} = \frac{C_{SO1}}{C_{SO2}}$$

If elements 1 and 2 are LPC elements but have partition coefficients with different orders of magnitudes, A depends on F; liquids with different values of C_{LO1}/C_{LO2} can be produced by different partial melting. Basalts experiencing further crystal fractionation derived from these different liquids plot on lines with different slopes A (Treuil and Varet, 1973; Treuil and Joron, 1975).

Considering HPC elements, it can be shown that for Ni the ratio C_{LO}/C_{SO} is almost independent of the extent of partial melting (F) and of the composition of

TABLE 2
Site 395, Hole 395, Trace-Element Data (expressed in ppm)

Element		Sc	Ti	V	Cr	Mn	Fe	Co		Ni		Cu	Zn
Analytical Method	Unit	NA	FX	FX	FX	FX	FX	FX	NA	FX	NA	AA	AA
Sample (Interval in cm)													
10, CC #1		8.25	180	49	2805	1007	69650	111	99.6	2160	1716	12	45
10, CC #2		1.92	240	3.6	323	542	26670	39	41.6	554	563	50	17
10, CC #3			540	34	1071	774	74620	104		1128		91	39
11-1, 105-107	A2*	38.4	10200	301	279	1548	80810	48	49.3	161	160	69	92
11-2, 62-64		36.6	9660	263.7	271	1394	83650	48	40.4	173	190	68	81
12-2, 109-111		37.3	9660	266	269	1394	83300	47	49.6	172	189	68	85
14-1, 112-114		40.8	10980	323	274	1548	96320	49	48.8		183	65	101
11-1, 131-132	A2*	37.3	9780	269	269	1316	83790	49	49.9	177	186	70	87
15-1, 71-73		38	9660	274	279	1316	82320	51	49.9		181	64	84
15-2, 130-133		37.9	9720	266	265	1316	85540	48	50.4	182	186	68	89
16-2, 104-105		36.9	9780	270	267	1394	85820	49	48.9	176	183	69	87
17-1, 50-69		35.2	2340	153	165	852	45640	40	43	155	170	0	19
18-1, 37-41	P1*	31.3	6060	217	361	1084	60340	38	41.3	139	152	68	53
18-1, 61-70		6.58	180	29	2677	852	71750	127	123	2370	2543	11	44
18-2, 33-38	P1*	30	6120	208	341	1084	58590	37	37.9	130	137	60	57
18-2, 85-95			240	52	4788	774	65520	116		2110		33	42
19-1, 18-20	A2*	38	9900	200	293	1472	77350	41	44	141	137	61	79
20-1, 32-36	P2*	30.6	7680	219	222	1084	66640	34	35	186	90	55	58

the presumed initial material. For Cr, the ratio C_{LO}/C_{SO} is somewhat dependent on F, increasing when partial melting increases, and is dependent on the composition of the presumed initial material (spinel content, for instance).

DISCUSSION AND INTERPRETATION OF RESULTS

From the shipboard data, we see that Ti and Zr behave similarly (Figure 4). It has been already shown that in mid-ocean ridge basalts, Ti behaves as an LPC trace element (Bougault, 1977). This is confirmed by the correlation shown on Figure 4. Leg 37 samples from Hole 332B plot on the same line as Leg 45 samples. The only difference between Leg 37 and Leg 45 samples is a shift along the line, both for phyric samples on one hand and aphyric samples on the other. This can be attributed either to a difference of range of the extent of partial melting or to a different initial mantle material. In the remainder of this section, we shall examine to what extent a difference can be determined for the extent of partial melting and/or the composition of initial mantle material between 23°N (Leg 45) and 36°N (FAMOUS area).

The hygromagmatophile elements with low partition coefficients—Ta, Hf, Tb, Zr, and Ti—have been plotted on Figures 5 through 9 as a function of Th. Th is thought to have the lowest partition coefficient among these elements. On the same figures, the field where the FAMOUS samples plot is shown and the dispersion indicated. Both Leg 45 and FAMOUS samples plot on straight lines passing through the origin, with dispersions more or less significant. For Leg 45 samples straight lines can be drawn because in fact each point represents an average value of many samples analyzed in the same unit.

The first striking feature is the different slopes between Leg 45 samples on the one hand and FAMOUS samples on the other. Leg 37 data are not included in the FAMOUS range, because they were determined by other laboratories and there may be a problem of reproducibility of trace elements among them. Even so, Leg 37 data for Th and Ta from other laboratories fall in the field of FAMOUS samples and not at all in the field of Leg 45 samples.

From the theoretical discussion presented earlier, *this has to be attributed to a difference between FAMOUS area and Leg 45 initial mantle materials.* Samples from Hole 396, which is roughly symmetric to Site 395 on the other (eastern) side of the Mid-Atlantic Ridge, plot very near the line defined for Site 395.

Of all the fields of FAMOUS samples presented on Figures 5 to 9, Ta versus Th (Figure 5) has the lowest dispersion. This is because Ta and Th have the lowest partition coefficients among the studied elements and, from our earlier discussion, the slope of the line relating these elements is not dependent on partial melting. The other elements plotted versus Th are LPC elements, but their partition coefficients are higher than those of Th and Ta. The slopes corresponding to given series of crystallization differentiation depend on the initial concentration in the liquid, that is to say on the extent of partial melting. This is why the dispersion for these elements is higher around "average lines."

Table 11A presents the values of slopes of a given LPC element i, plotted against other LPC elements j,

TABLE 2 – *Continued*

Rb	Sr	Zr	Sb	Cs	La	Eu	Tb	Hf	Ta	Th
NA	FX	FX	NA	NA	NA	NA	NA	NA	NA	NA
	6	3	<27	0.189	<0.027	<0.84	≤0.057	<0.014	<0.14	<0.008	0.05
	99	8	<14		<0.015	0.11	0.15	0.008	<0.067	<0.004	0.015
	4	4									
3.3	127	121	112	0.50	0.099	3.25	1.5	0.87	2.84	0.200	0.137
<1.4	119	112	126	0.020	0.024	3.2	1.33	0.82	2.71	0.183	0.132
<0.9	120	119	120	0.016	0.037	2.12	1.42	0.83	2.73	0.194	0.137
4.1			137	0.98	0.027	3.6	1.49	0.93	3.18	0.207	0.141
2.4	120	114	136	0.017	0.08	3.1	1.36	0.84	2.86	0.193	0.134
<1.1			108	0.018	0.05	4.1	1.40	0.83	2.83	0.192	0.138
1.9	118	116	112	0.015	0.020	3.4	1.45	0.85	2.88	0.187	0.130
<1.8	118	120	108	0.033	0.036	3.3	1.40	0.83	2.83	0.190	0.130
3.8	324	16	<27	0.017	0.34	0.44	0.41	0.193	0.19	<0.057	<0.019
2.1	112	67	63		0.038	2.04	0.95	0.52	1.65	0.103	0.079
<1.8	6	4	<25	0.018	<0.02	0.12	<0.05	0.011	<0.13	<0.007	<0.027
2.3	114	67	68	0.033	0.066	1.9	0.97	0.54	1.66	0.109	0.083
	10		1								
<1.5	130	127	131	0.026	0.040	3.8	1.42	0.84	3.00	0.201	0.154
8.1	162	94	98	0.101	0.40	2.77	1.18	0.64	2.21	0.149	0.113

both for FAMOUS and Leg 45 samples. The major differences between Leg 45 and FAMOUS samples are shown by comparing slopes (i versus j) when i or j corresponds to Ta or Th (the lowest partition coefficient elements). Table 11B also shows absolute values of LPC elements for both Leg 45 and FAMOUS aphyric basalts (Unit A_3 and Sample ARP 7-7, respectively) and plagioclase phyric basalts (Unit P_2 and Sample ARP 31-36, respectively). One can observe that for both types of basalts, Th and Ta values are lower, and other LPC elements are higher for Leg 45 samples than they are for FAMOUS samples. *This confirms that there is a difference between the initial mantle compositions of these areas*; whatever the partial melting or crystallization processes involved, it would not be possible after partial melting and crystallization to have some LPC elements lower and others higher if the mantle had the same initial composition in both cases.

For Leg 45 samples, it is not possible to determine differences in the extent of partial melting on the basis of LPC elements, because of the steep slopes of the lines and the analytical precision that would be required. Nevertheless, this can partly be shown through Cr and Ni data.

Log Cr versus log Ni is plotted on Figure 10. Leg 37 and FAMOUS samples define two common fields: one for aphyric samples, the other for plagioclase-phyric samples. Since the Ni concentration in the liquid is almost independent of partial melting and the CR concentration is somewhat dependent, these trends are mainly representative of crystallization history. The FAMOUS aphyric field is narrow, but cannot be resolved to a straight line because of variations in the proportions of crystallizing minerals. The FAMOUS plagioclase-phyric field is above and larger than the aphyric field, probably because of the variable content of clinopyroxene phenocrysts (the partition coefficient of Cr in clinopyroxenes is higher than 10). But the clinopyroxene content of FAMOUS plagioclase-phyric basalts is not at all sufficient to account for their high Cr concentrations relative to FAMOUS aphyric basalts for a given value of Ni. This is because the Cr concentration in the liquid increases with partial melting, as discussed theoretically earlier. In this respect, plagioclase-phyric basalts appear to derive from liquids produced by a higher degree of partial melting than aphyric basalts. This is in agreement with LPC element abundances, which are generally higher for plagioclase-phyric basalts than for aphyric basalts.

On Figure 10, both the fields of plagioclase-phyric basalts of Site 395 and 396 and of aphyric basalts, except A_3 and A_4 Sample 67-2, 54-59 cm, are shifted compared with FAMOUS and Leg 37 data. The different relative positions of the various Leg 45 aphyric basalts and the plagioclase phyric basalts is a consequence of different degrees of partial melting and of different proportions of crystallizing minerals. A plot of Ni or Cr versus an LPC element would result in a similar conclusion about partial melting; at least two and probably three different degrees of partial melting are represented.

It is somewhat difficult to draw conclusions about crystallization processes with Leg 45 samples, because of the low number of different rock types we have, compared with FAMOUS-Leg 37 data, and because of the different degrees of partial melting. Nevertheless, it

TABLE 3
Site 395, Hole 395A, Major Element Data (volatile-free concentrations, wt. %)

Unit		A2						P2								P3						P4							P5			
Sample (Interval in cm)	4-1, 91-113	5-1, 100-103	6-1, 130-134	7-1, 76-82	8-1, 50-52	9-2, 18-21	11-1, 117-129	13-1, 106-110	14-1, 92-99	14-2, 98-112	14-2, 98-112	15-1, 93-102	15-2, 102-108	15-3, 128-142	15-5, 0-11	16-1, 69-74	16-1, 90-98	16-1, 100-104	17-1, 115-124	18-1, 140-146	20-1, 43-45	22-1, 87-92	22-2, 72-76	23-1, 65-68	23-1, 117-122	23-1, 145-147	24-1, 125-129	26-1, 129-133	27-1, 127-131	28-1, 116-122	29-1, 119-122	30-1, 82-87	31-1, 63-67
Depth (m)	105	115	116	124	134	143	163	182	188	190	190	195	197	199	201	210	210	210	220	229	240	258	260	269	270	270	278	298	306	317	327	335	344
Rock Type	G	aphy. B	aphy B	aphy. B	aphy B	aphy. B	aphy B	pl ol. B	pl. ol. B	pl. ol B	pl. ol. B (altered)	pl. ol. B	pl ol B	pl. ol B	pl. ol B	pl. ol B	pl ol pyr B	pl. ol. pyr. B	pl. ol. pyr B	pl ol. pyr B	pl ol. pyr B	pl ol. pyr B	pl. ol. pyr B	pl. ol pyr. B	pl ol pyr. B	pl ol. pyr B	pl ol pyr. B	pl. ol pyr B	pl. ol. pyr B	pl. ol. B	pl. ol. pyr B	pl. ol. B	pl. ol. pyr B
SiO_2	51.6	49 4	49.6	49 4	49 1	49 4	49 8	49 9	49 2	49 5	49.0	49 7	50 2	49 9	49 1	50.3	48 8	49 5	49 9	49.4	49.6	49.6	50 1	49 4	50.1	49 1	49.7	49.6	49.6	49.6	49 1	49 3	49 7
Al_2O_3	18.86	14.87	15.19	14 92	14 89	15 14	15.06	18.64	17 81	18 28	17.93	18.25	17 97	17 72	19 17	17.74	17 84	17 36	17 84	17 57	17 71	17 8	16 25	17 54	17.65	17 33	17 76	17.20	16 90	18 61	18 13	17.69	18 59
Fe_2O_3 (t)	7.11	12.20	12.03	12 27	12.49	12 20	12.65	8.37	9 43	8 94	9.24	9 40	9 73	9.91	8.49	9.61	8 94	8.67	8 49	8.58	9.20	8.73	9 32	9 24	8.51	8 24	8.69	8.76	8 84	8.56	8.71	8.8	8 67
FeO		8.07				8 38			6 34				5 78		7 0				4.51				5 65								5.11		4 06
MnO	0.13	0.18	0.18	0.18	0.20	0.18	0.19	0.14	0 14	0.13	0.15	0.14	0 14	0.15	0.13		0.14	0.14		0.14	0 15	0.13	0 15	0 15	0.14	0 14	0.14	0.14	0 14	0 15	0.14	0 13	0 13
MgO	5.5	8.8	8.5	8 4	8 4	8 5	8.6	6.5	7 1	6 9	6.1	7 3	6 8	7 3	7 0	6.7	7.5	7 8	7.2	7 3	8 0	8 0	8 4	7 6	8.4	8 5	7 8	7 9	8 3	6.6	7.2	8 3	6 8
CaO	12.42	10.53	10.60	10 61	10.49	10 65	10 74	12.62	11.97	12 10	12.11	12 10	12.01	12 15	12.16	12.01	12.67	12.57	12.82	12.68	12.85	12 91	12 39	12 39	12 39	12 26	12 50	12 21	12 11	12 27	12 26	11 92	12 33
Na_2O	4 03	2 9	2 85	2 83	2.85	2.83	2.79	2.75	2 73	2 88	2.88	2 72	2 94	2.82	2 72	2.87	2 32	2.42	2 34	2 42	2 42	2 34	2 42	2 62	2.54	2 39	2.59	2.42	2 57	2 74	2 62	2 62	2 77
K_2O	0.10	0.10	0.16	0 17	0 13	0.11	0.16	0.15	0 11	0 08	0.20	0 09	0.10	0.11	0.07	0.18	0.12	0.12	0 12	0.11	0 16	0.10	0 08	0 25	0.16	0 11	0.10	0.06	0 06	0 15	0.21	0 09	0.17
TiO_2	0.81	1.62	1 64	1 63	1.64	1.64	1.65	1.39	1 36	1 33	1.36	1 34	1 39	1.37	1.16	1.40	1.05	1.07	1.04	1 05	1.07	1.02	1 13	1 12	1.11	1 07	1.12	1.13	1 13	1 19	1 25	1 15	1 17
P_2O_5	0 17	0.17	0 19	0 17	0.16	0 16	0 18	0.16	0 14	0 15	0.14	0 14	0 14	0.14	0 14		0 12	0.12		0 11	0 11	0.11	0.09	0 11	0.11	0 12	0 11	0 11	0 10	0 12	0 14	0 10	0 12
Total	100 73	100.77	100 74	100.58	100.35	100.81	100.82	100.48	99 99	100 29	99.11	101 18	101 42	101 57	100 14	100.81	99 50	99.77	99.75	99 36	101.27	100 74	100.33	100 52	101.11	99.26	100 51	99.53	99 75	99 99	99 76	100 10	100 45
Lol	-1 1	-0.9	-1 9	-1 0	-0.1	-0.7	-1.3	-2.1	-1 6	-1 8	-2.0	-1 9	-2.1	-1.2	-1.4	-2.0	-0 7	-0.5	-2.0	-1 7	-0 4	-1.9	-1.6	-0 9	-0.7	-0.6	-0 9	-1.7	-1.6	-1.4	-1 2	-1.7	-2.5

Note G = gabbro, B = basalt, aphy = aphyric, pl = plagioclase, ol = olivine, pyr = clinopyroxene, Dol = dolerite.

TABLE 3 – *Continued*

Unit	P5					A3												A4				P4'	A4	P4'			A4			A4
Sample (Interval in cm)	31-1, 70-76	32-1, 54-62	32-1, 54-62	32-2, 56-63	33-2, 9-13	33-2, 127-129	35-1, 53-54	37-1, 136-141	39-1, 102-107	41-1, 142-144	42-1, 86-89	45-1, 124-127	47-1, 63-67	48-2, 135-140	49-2, 13-17	51-2, 41-44	52-1, 48-53	53-1, 7-11	55-1, 49-54	56-2, 75-81	57-1, 125-131	58-2, 115-122	59-2, 65-69	60-3, 137-143	61-2, 37-45	62-1, 40-42	62-1, 80-87	63-1, 108-116	64-2, 116-122	64-3, 48-53	65-1, 81-86	66-2, 66-71	67-2, 54-59
Depth (m)	344	352	352	353	362	364	381	401	420	438	446	475	492	504	512	530	539	542	558	568	579	589	598	608	617	521	521	524	535	536	546	556	567
Rock Type	pl. ol. B	breccia matrix	breccia clast	breccia clast	pl. ol. B	aphy. B	aphy B	aphy. B	aphy. B	aphy. B	aphy. B	aphy. B	aphy. B	aphy. B	aphy B	aphy B	aphy B	aphy. B	aphy B	aphy B	aphy B	glass	aphy B	aphy B	pl ol pyr Dol	aphy. B	pl ol pyr Dol	pl ol pyr Dol	pl ol pyr Dol	aphy. B	aphy. B	aphy B	aphy B
SiO_2	49 1	49.0	49 6	49.2	50 0	49 7	49 8	49 9	49 9	49.7	49 7	49 8	49 8	49 4	49.6	49 8	49 8	49 6	49.3	49 9	49 2	50 5	49.0	48 8	49 5	48 6	49 6	49 5	49 3	49.2	48.7	49 1	49 9
Al_2O_3	18 42	18.25	18 79	18 94	18 44	15 29	15 14	15.06	15 33	15.07	15.19	15.09	15 81	15.09	15.08	15.08	15 03	15 11	14.88	14 88	15 14	14 47	15.24	15 15	16 96	15 06	16 30	17 44	16 91	15 27	15.12	15 24	15 10
Fe_2O_3 (t)	8.69	8.09	8.73	8.3	8 89	11.07	11 13	10 90	10.98	11.17	11.42	11.45	11.05	11.16	11 14	11.34	11.61	11.28	11.13	11 13	11.20	10 86	11 25	11 39	8.97	11.15	9 05	8 59	8.85	11 60	11.45	11 65	10.56
FeO							7 33					7.41							6.21				6 26			6.11	4 93			4 96		5 95	5 08
MnO	0.14	0.15	0.13	0.15	0.14	0.18	0 18	0.17	0.18	0.19	0.19	0 19	0.18	0 19	0.18	0.19	0 19	0.18	0.17	0 18	0 18	0.18	0 18	0 20	0.14	0 18	0 15	0.15	0.14	0 20	0.20	0 20	0.17
MgO	7 0	5 9	5 5	7 1	7 3	7 7	7 7	7.5	7 6	7.5	7.4	7.3	7 2	7 9	8 1	7.5	7 3	7 9	8.0	7 8	8 1	8 2	8.1	8 4	8 3	8.5	8 1	8 5	8 5	8.6	8.2	8 3	7 3
CaO	12.31	15 64	13 90	12.38	12.53	11 33	11 29	11.24	11.39	11.25	11 23	11 27	11.52	11.23	11 32	11.33	11 47	11 22	11.18	11 18	11 09	10 50	11.18	11 12	11.93	11 09	11 98	12 16	12.06	10 87	11 23	11 17	11 40
Na_2O	2.72	2 62	2 77	2 69	2 74	2 72	2 74	2.72	2 72	2.65	2 69	2 62	2.65	2 77	2 72	2.59	2.72	2 69	2.72	2.72	2 62	2 65	2.65	2.57	2.44	2.92	2 44	2 42	2.44	2 49	2.72	2 69	2 72
K_2O	0.17	0 36	0.15	0 12	0 17	0 24	0 18	0 29	0 28	0 27	0 16	0 18	0 21	0 25	0 17	0 23	0 18	0 18	0 17	0 17	0 22	0 10	0 30	0 17	0 07	0 22	0 12	0 07	0 11	0 25	0 23	0 20	0 29
TiO_2	1.14	1.09	1 19	1.09	1 13	1 70	1 71	1.70	1 72	1.74	1.75	1.76	1.67	1 71	1 72	1.72	1 74	1 72	1.73	1 74	1.59	1 58	1.59	1 59	1.14	1 59	1 18	1 08	1.10	1 63	1.63	1 64	1.69
P_2O_5	0.11	0.12	0 11	0 10	0 09	0 17	0 17	0 16	0 17	0.18	0 17	0 17	0.16	0.17	0 18	0.17	0 20	0.17	0.17	0 16	0 15	0 12	0.15	0 14	0.10	0 15	0 11	0 09	0.09	0 16	0.15	0 15	0 15
Total	99.80	101.22	100.87	100.05	101.43	100 10	100 04	99 54	100.27	99.72	99.90	99.83	100.25	99.87	100.21	99.95	100 24	100.05	99.32	99.76	99.49	99.16	99.64	99 53	99.55	99.46	99 03	100 00	99.50	100 27	99.63	100 34	99.28
Lol	-2.4	-7.7	-3.1	-1.9	-2.1	-1.7	-1.1	-1.9	-1.9	-1.3	-0.8	-1 1	-1.2	-1.5	-1.2	-1.3	-1.0	-1 3	-1.6	-1 9	-2 3	-0.5		-1 9	-1.8	-1 9	-1.8	-1 8	-2.0	-4.9	-2.1	-2 6	-2.6

TABLE 4
Site 395, Hole 395A, Trace-Element Data (expressed in ppm)

Element		Sc	Ti	V	Cr	Mn	Fe	Co		Ni		Cu	Zn	Rb	Sr	Zr	Sb	Cs	La	Eu	Tb	Hf	Ta	Th
Analytical Method	Unit	NA	FX	FX	FX	FX	FX	FX	NA	FX	NA	AA	AA	NA	FX	FX	NA	NA	NA	NA	NA	NA	NA	NA	NA
Sample (Interval in cm)																								
4-1, 91-113	G	33.7	4860	233	247	1007	49770	29	30.7	124	128	73	50	2.1	178	36	59	0.030	0.215	2.3	1.61	0.75	1.17	0.034	0.023
5-1, 100-103		37.0	9720	270	272	1394	85400	50	50.5	173	197	77	81	<1.8	121	113	123	0.020	0.038	3.1	1.33	0.82	2.85	0.189	0.149
6-1, 113-134		34.2	9840	271	274	1394	84210	50	45.6	177	168	73	84	1.9	122	107	105	0.012	0.04	3.3	1.29	0.71	2.52	0.174	0.129
7-1, 76-82	A2	36.9	9780	271	273	1394	85890	48	49.	186	178	70	84	2.3	122	111	105		0.10	3.3	1.4	0.82	2.72	0.197	0.136
8-1, 50-52		37.1	9840	265	264	1594	87430	49	48.8	178	184	72	87	2.7	117	111	104	0.043	0.018	3.2	1.45	0.83	2.85	0.196	0.131
9-2, 18-21		37.1	9840	271	269	1394	85400	50	48.7	193	185	72	83	3.2	120	112	115	0.102	0.021	3.2	1.46	0.85	2.87	0.190	0.124
11-1, 117-129		37.5	9900	270	268	1471	88550	50	49.7	176	184	73	86	2.2	124	108	143	0.012	0.036	3.4	1.42	0.88	2.91	0.187	0.110
13-1, 106-110		33.1	8340	241	232	1084	58590	40	44.0	134	128	62	69	2.9	165	98	109		0.12	2.9	1.29	0.70	2.47	0.171	0.107
11-1, 92-99		32.9	8160	234	236	1084	66010	39	38.0	88	104	59/61	63/64	<1.3	160	97	109	0.017	0.048	3.0	1.22	0.68	2.39	0.163	0.117
11-2, 98-112		32.8	7980	232	228	1007	62580	36	39.5	89	105	59	63	3.7	162	95	125	0.042	0.175	2.9	1.24	0.71	2.48	0.162	0.131
14-2, 98-112	P2	32.2	8160	234	236	1162	64680	38	38.3	110	99	61	65	<0.9	171	99	106	0.008	0.02	2.90	1.26	0.66	8.29	0.16	0.117
15-1 93-102 alt		32.1	8040	229	234	1084	65800	37	38.4	98	99	61	63	1.7	160	100	95		0.055	3.04	1.21	0.69	2.26	0.160	0.104
15-2, 102-108		32.5	8340	236	230	1084	68110	36	37.3	93	94	59	61	<1.8	155	97	88	0.012	0.030	3.0	1.21	0.68	2.29	0.155	0.129
15-3, 128-142		32.3	8220	239	228	1162	63370	37	39.1	91	106	62	65	<1.8	160	97	102	0.012	0.057	3.1	1.27	0.67	2.38	0.157	0.136
15-5, 0-11		28.1	6960	202	252	1007	59430	37	35.9	95	104	59	51	<1.5	158	84	92	0.010	0.025	2.4	1.06	0.58	2.04	0.138	0.107
16-1, 69-74			8400	240	226		67270	37		104		63	63		202	93									
16-1, 90-98		30.9	6300	220	342	1084	62580	38	39.9	134	136	63	58	2.6	115	66	77	0.186	0.0100	2.2	0.93	0.54	1.74	0.114	0.083
16-1, 100-104		32.4	6420	221	362	1084	60690	39	42.7	144	156	70	59	2.2	115	66	69	0.048	0.068	2.2	1.01	0.57	1.76	0.111	0.084
17-1, 115-124	P3	32.	6240	220	348		59430	38	40.5	144	146	63	53	2.	122	67	82	0.020	0.13	3.2	1.01	0.56	1.80	0.113	0.103
18-1, 140-146		30.9	6300	224	344	1084	60060	40	39.7	136	133	68	63	2.5	118	64	72	0.071	0.128	2.0	0.93	0.54	1.70	0.113	0.074
20-1, 43-45		32.4	6420	223	358	1162	64400	39	41.4	141	144	63	63	2.6	117	69	74	0.055	0.043	2.02	1.00	0.56	1.75	0.115	0.091
22-1, 87-92		30.4	6120	223	354	1007	61110	39	39.5	152	149	68	58	2.1	115	70	64		0.132	1.81	0.92	0.52	1.63	0.103	0.067
22-2, 72-76		33.4	6780	237	368	1162	65240	40	42.1	137	145	73	64	1.8	136	71	74	0.013	0.062	2.1	0.99	0.56	1.81	0.116	0.100
23-1, 65-68		32.1	6720	228	367	1162	64680	38	39.2	124	129	72	64	6.9	138	80	80	0.140	2.90	2.22	1.02	0.57	1.94	0.109	0.081
23-1, 117-122		31.3	6660	218	375	1084	59570	40	40.3	147	151	67	66	2.2	138	75	90	0.023	0.083	2.3	1.05	0.55	1.85	0.106	0.105
23-1, 145-147	P4	30.9	6420	263	279	1084	57680	40	41.8	149	169	66	68	<1.3	127	73	79	0.019	0.035	2.1	1.01	0.55	1.83	0.105	0.076
24-1, 125-129		32.	6720	225	229	1084	60830	37	41.2	136	146	67	61	1.3	135	72	75		0.040	2.4	0.99	0.56	1.80	0.111	0.068
26-1, 129-133		32.1	6780	224	315	1084	61320	41	39.3	127	130	67	60	1.8	134	70	86	0.013	0.028	2.21	1.03	0.58	1.95	0.107	0.075
27-1, 127-131		33.	6780	224	314	1084	61880	40	43.1	129	150	71	72		133	64	92	0.188	0.035	2.32	1.06	0.58	2.00	0.114	0.079
28-1, 116-122		28.9	7140	206	284	1162	59920	38	38.7	148	144	57	69	2.1	168	81	95	0.031	0.167	2.6	1.07	0.57	2.01	0.126	0.0111
29-1, 110-122		31.3	7500	215	295	1084	60970	38	38.1	127	140	57	65	4.3	158	80	84	0.047	0.168	2.7	1.14	0.64	2.15	0.137	0.101
30-1, 82-87		30.8	6900	202	293	1007	61600	38	41.4	142	169	63	63	<1.3	158	76	96	0.016	0.063	2.5	1.08	0.58	1.97	0.126	0.095
31-1, 63-67		29.9	7020	200	208	1007	60690	38	38.9	134	140	59	66	3.6	165	82	92	0.079	0.243	2.4	1.06	0.57	1.98	0.124	0.112
31-1, 70-76	P5	29.9	6840	200	288	1084	60830	37	39.3	131	144	59	60	4.2	172	81	88		0.21	2.3	1.08	0.56	1.87	0.121	0.088
32-1, 54-62		27.6	6540	232	299	1162	56630	35	35.5	165	145	49	48	9.1	172	70	74	0.240	0.440	2.11	0.95	0.51	1.69	0.111	0.080
32-18, 54-62		30.9	7140	193	255	1007	61110	36	38.3	111	116	59	59	5.5	177	80	84	0.147	0.43	2.4	1.07	0.58	2.03	0.124	0.074
32-2, 56-63		29.2	6540	200	260	1162	58100	36	36.8	121	134	62	62	3.3	180	76	77	0.018	0.141	2.3	1.02	0.54	1 88	0.116	0.080
33-2, 9-13		30.1	6780	218	304	1084	62230	37	38.9	135	135	62	61	3.5	162	69	77	0.033	0.221	2.2	1.02	0.57	1.86	0.115	0.087
33-2, 127-129		38.2	10200	303	258	1394	77490	43	43.2	114	118	59	79	2.9	132	118	124		0.018	4.3	1.50	0.85	3.02	0.219	0.153
35-1, 53-54		39.4	10260	311	260	1394	77910	43	43.5	113	123	61	79		129	127	122	0.040	0.030	4.0	1.55	0.91	3.18	0.232	0.142
37-1, 136-141		38.3	10200	308	260	1316	76300	45	44.3	121	122	56	76	4.7	135	117	142		0.28	4.4	1.50	0.85	3.10	0.224	0.157
39-1, 102-107		40.7	10320	304	251	1394	76860	41	43.3	128	128	57	84	3.1	129	122	137	0.055	0.175	4.0	1.51	0.85	3.14	0.216	0.146
41-1, 142-144	A3	39.1	10440	303	249	1471	78190	43	44.7	121	119	57	81	4.4	130	128	129		0.21	4.0	1.55	0.93	3.19	0.236	0.175
42-1, 86-89		38.8	10600	302	243	1471	79940	44	43.2	115	114	61	81	<1.5	132	131	148	0.050	<0.02	4.0	1.52	0.92	3.28	0.230	0.21
45-1, 124-127		38.9	10660	308	243	1471	78890	44	43.7	111	116	54	92	2.8	131	131	123		<0.02	4.2	1.55	0.90	3.20	0.236	0.158
47-1, 63-67		38.4	10020	302	258	1394	80640	42	42.2	119	117	56	80	<1.5	134	118	123	0.072	<0.02	4.0	1.43	0.87	3.02	0.220	0.152
48-1, 135-140		38.3	10260	302	250	1471	78610	42	44	120	120	57	90	3.6	131	124	122		0.081	4.1	1.48	0.87	3.04	0.227	0.163
49-2, 13-17		39.5	10320	305	257	1394	79240	45	44.5	118	252	59	86	2.3	128	128	135	0.036	<0.024	4.1	1.60	0.90	3.33	0.231	0.161
51-2, 41-44		37.9	10320	302	251	1471	79310	41	42.8	119	116	60	90	<1.5	130	128	137	0.039	0.023	3.9	1.49	0.89	3.19	0.225	0.164
52-1, 48-53		38.3	10440	305	251	1471	81270	42	42.6	118	115	61	116	2.2	134	123	144	0.038	0.029	4.0	1.52	0.90	3.2	0.224	0.152
53-1, 7-11		38.2	10320	309	241	1394	78960	40	42.6	119	118	56	92	2.5	131	128	136	0.036	0.015	3.9	1.53	0.88	3.16	0.229	0.174
54-1, 48-51		38.3	10320	314	245	1316	77770	41	43.4	111	114	57	83	<1.5	124	132	131	0.032	0.013	4.0	1.51	0.90	3.22	0.227	0.186
55-1, 49-54		38.9	10380	312	249	1394	77910	44	44.3	116	118	57	92	5.4	131	126	124		0.20	4.1	1.55	0.91	3.19	0.241	0.164
56-2, 75-81			10340	311	246		77910	43		102		57	103		131	129									
57-1, 125-131		37.4	9540	288	302	1394	78400	47	48.2	163	177	63	83	4.7	134	105	116	0.28	0.168	3.6	1.42	0.82	2.85	0.190	0.141
58-2, 115-122	A4		9480	273	294	1394	76010	45		169		62	79		119	110									
59-2, 65-69		36.6	9540	279	298	1394	78750	46	47.5	177	182	69	83	4.6	127	111	110	0.022	0.11	3.4	1.43	0.80	2.79	0.194	0.159
60-3, 137-143		36.9	9540	285	206	1549	79730	48	46.9	174	171	68	81	3.1	130	119	118	0.0148	0.089	3.4	1.38	0.81	2.78	0.194	0.131
61-2, 37-45	P4'	32.4	6840	238	219	1084	62790	39	40.8	133	137	69	65	<1.2	129	86	77		0.02	2.2	1.08	0.58	1.87	0.111	0.080
62-1, 40-42	A4	36.5	9540	282	316	1394	78050	48	48.7	179	183	69	90	3.6	128	117	117	0.019	0.144	3.5	1.37	0.80	2.87	0.195	0.144
62-1, 80-87		33.2	7080	251	308	1162	63340	38	41	116	133	68	64	3.	129	74	82	0.021	0.126	2.35	1.09	0.61	1.99	0.111	0.082
63-1, 108-116	P4'	29.7	6480	211	362	1162	60130	38	37.6	129	140	61	69	<0.8	132	68	64		0.026	2.02	0.94	0.52	1.66	0.100	0.069
64-2, 116-122		31.6	6600	217	330	1084	61950	39	41	144	149	61	63	2.6	139	66	74	0.022	0 148	2.1	1.02	0.56	1.81	0.103	0.064
64-3, 48-53		36.4	9780	267	294	1549	81200	47	47.4	180	181	57	82	6.7	126	108	129	0.079	0.171	3.7	1.37	0.82	2.85	0.198	0.146
65-1, 81-86	A4	36.9	9780	277	298	1549	80150	47	48.0	170	177	62	86	5.4	130	114	111	0.039	0.174	3.6	1.42	0.82	3.07	0.197	0.158
66-2, 66-71		37.1	9840	275	295	1549	81550	45	46.9	158	171	62	87	4.6	131	106	110	0.047	0.172	3.5	1.40	0.83	2.88	0.200	0.138
67-2, 54-59	A4	37.8	10140	297	263	1316	73920	44	43.8	129	131	54	83	3.1	132	124	112	0.019	0.144	4.0	1.46	0.87	3.07	0.225	0.142

can be stated that none of the units mentioned can be considered to represent primary liquids (Ni values should be around 250 ppm). If, however, we can consider that Leg 45 plagioclase-phyric samples are derived from the same, or similar, initial liquids, both HPC and LPC elements allow us to infer that the *extent* of crystal fractionation increases in the order P_3, P_4, P_5, and P_2.

CONCLUSIONS

1. *Trace element* data are consistent with the classification of chemical units determined on Leg 45 from major-element shipboard study.

2. *Alkali metals* show significant variations in all the samples studied. Notably, Cs = f (Rb), and, within a given unit Cs = f (K_2O). This is the result of *secondary processes (alteration).*

3. From high-partition-coefficient and low-partition-coefficient elements, it can be concluded that none of the basaltic samples recovered can be considered as primary liquids and all have undergone a *substantial history of crystallization.*

4. Except for Units P_3, P_4, and P_5, which can have been derived from a single parental magma, the different units derive from different magmas obtained by *different degrees of partial melting.*

TABLE 5
Site 396, Hole 396, Major-Element Data (volatile-free concentrations, wt. %)

Unit	Pa	Pb				Pc			
Sample (Interval in cm)	14-6, 20-45	15-4, 48-53	16-3, 137-142	18-1, 130-136	19-2, 138-141	22-4, 144-150	23-1, 143-147	24-3, 73-78	25-1, 96-100
Depth (m)	125	135	144	160	173	201	209	219	221
Rock Type	pl. ol. B	pl. ol. B	pl. ol. B	pl. ol. B	pl. ol. B	pl. ol. B	pl. ol. B	pl. ol. B	pl. ol. B
SiO_2	49.3	49.5	49.8	49.7	49.7	49.8	49.2	49.1	49.7
Al_2O_3	16.25	16.75	16.73	16.93	16.70	16.93	16.68	16.58	16.71
Fe_2O_3 (t)	9.96	9.17	9.24	9.68	9.23	9.47	9.29	9.68	9.49
FeO	5.36	4.36	4.45			4.64		5.23	
MnO	0.16	0.15	0.15	0.17	0.17	0.15	0.15	0.16	0.15
MgO	7	8.5	8.1	7.9	7.7	7.6	7.3	7.9	7.4
CaO	11.57	11.88	11.95	12.09	11.98	12.11	11.96	12.07	11.99
Na_2O	2.62	2.59	2.57	2.62	2.73	2.69	2.72	2.65	2.65
K_2O	0.31	0.21	0.24	0.29	0.21	0.25	0.21	0.23	0.13
TiO_2	1.50	1.24	1.27	1.27	1.29	1.29	1.29	1.29	1.29
P_2O_5	0.15	0.12	0.12	0.13	0.13	0.11	0.11	0.12	0.11
Total	98.82	100.11	100.17	100.78	99.84	100.30	98.91	99.78	99.62
Lol	-2.0	-3.1	-2.4	-2.6	-3.0	-2.3	-2.5	-2.0	-2.2

Note: pl = plagioclase, ol = olivine, B = basalt.

From low-partition-coefficient hygromagmatophile elements, it can be stated, for Sites 395 and 396, that the initial mantle materials are similar, if not exactly the same. The *initial mantle material at 23°N* (Leg 45) is *different from the initial mantle material at 36°N* (FAMOUS area). This is the most important result of this study, which demonstrates mantle heterogeneity.

REFERENCES

Allegre, C. J., Javoy, M., and Michard, G., 1968. Etude de l'abondance des éléments de transition dans l'écorce terrestre, comparée à celle des terres rares. *In* Ahrens, L. H. (Ed.), *Origine et Distribution des Eléments*: London.

Ahrens, L. H. (Ed.), (Pergamon Press), p. 914-928.

Bougault, H., 1977. First transition series elements fractional crystallization and partial melting. *In* Aumento, F., Melson, W. G., et al., *Initial Reports of the Deep Sea Drilling Project*, v. 37, Washington (U.S. Government Printing Office), p. 539-546.

Bougault, H. and Hekinian, R., 1974. Rift valley in the Atlantic Ocean near 36°50′N: petrology and geochemistry of basaltic rocks, *Earth Planet. Sci. Lett.*, v. 24, p. 249-261.

Bougault, H., Cambon, P., and Toulhoat, H. (1977). X-ray spectrometric analysis of trace elements in rocks; correction for instrumental interferences, *X-Ray Spectrometry*, v. 6, no. 2, p. 66-72.

Burns, R. G., 1970. *Mineralogical applications of crystal field theory*: Cambridge. (Cambridge Earth Sciences Series).

Curtis, C. D., 1964. Application of the crystal field theory: the inclusion of trace transition elements in minerals during magmatic differentiation, *Geochim. Cosmochim. Acta*, v. 28, p. 389-403.

Hart, S. R., 1971. Rb, Cs, Sr, and Ba contents, and Sr isotopic values of ocean floor basalts, *Phil. Trans. Roy. Soc. London*, ser. A., v. 268, p. 573-587.

Orgel, L. E., 1964. Chimie des éléments de transition. Dunod Ed., Paris.

Peck, L. C., 1964. Systematic analysis of silicates, *Geological Survey Bulletin 1170*: Washington (U.S. Government Printing Office).

Shaw, D. M., 1970. Trace elements fractionation during anatexis, *Geochim. Cosmochim. Acta*, v. 34, p. 237-243.

Treuil, M. and Joron, M., 1975. Utilisation des éléments hygromagmatophiles pour la simplication de la modelisation quantitative des processus magmatiques: exemple de l'AFAR et de la dorsale medio-atlantique. *Societa Italiana Mineralogia et Petrologia*, v. 31, p. 125-174.

_____, 1976. Etude geochimique des éléments en trace dans le magmatisme de l'Afar. Implication petrogénétique et comparaison avec le magmatisme de l'islande et de la dorsale medio-atlantique. Inter-u. ion Commission on Geodynamics: *Scientific Report 16*. Proceedings of an international symposium on Afar region and related rift problems, Bad Bergrabern F. R. Germany, April 1-6 1974.

Treuil, M. and Varet, J., 1973. Critères volcanologiques petrologiques et geochimiques de la génèse et de la différenciation des magmas basaltiques: exemple de 'AFAR, *Bull. Soc. Geol. France*, v. 15, p. 506-540.

TABLE 6
Site 396, Hole 396, Trace-Element Data (expressed in ppm)

Element	Sc	Ti	V	Cr	Mn	Fe	Co		Ni		Cu	Zn	Rb	Sr	Zr	Sb	Cs	La	Eu	Tb	Hf	Ta	Th
Analytical Method	NA	FX	FX	FX	FX	FX	FX	NA	FX	NA	AA	AA	NA	FX	FX	NA	NA	NA	NA	NA	NA	NA	NA	NA
Sample (Interval in cm)																							
Unit P_a																							
14-6, 20-25	36.8	9000	312	288		69720	40	40.7	111	114	58	73	4.7	148	109	118	0.021	0.260	3.5	1.38	0.79	2.64	0.207	0.161
Unit P_b																							
15-4, 48-53		7440	256	415		64190	41		171		65	66		155	86									
16-3, 137-142	34.8	7620	268	397		64680	40	40.8	143	142	64	67	4.4	155	90	90	0.020	0.250	3.0	1.14	0.64	2.14	0.167	1.22
18-1, 130-136		7620	262	371		67760	40		142		67	66		146	87									
19-2, 138-141	35.4	7740	269	391		64610	39	41.4	142	144	67	65	3.9	168	86	83	0.025	0.255	2.9	1.23	0.66	2.24	0.173	0.132
21-1, 87-89		7140	261	431		62650	41		189		67	65		150	85									
Unit P_c																							
22-4, 144-150	34.5	7740	254	284		66290	40	41.5	123	121	65	70	5.1	135	86	103	0.014	0.289	2.65	1.23	0.67	2.16	0.153	0.116
23-1, 143-147	34.2	7740	255	208		65030	41	42.4	128	125	65	72	4.2	133	93	89	0.011	0.228	2.7	1.19	0.67	2.16	0.152	0.096
24-3, 73-78	35.1	7740	254	293		67760	41	42.8	124	1340	66	73	4.3	128	86	90	0.025	0.234	2.7	1.26	0.68	2.31	0.156	0.116
25-1, 96-100	34.9	7740	259	288		66430	40	40.9	109	116	64	71	3.0	130	81	107	0.016	0.056	2.7	1.20	0.68	2.18	0.153	0.126

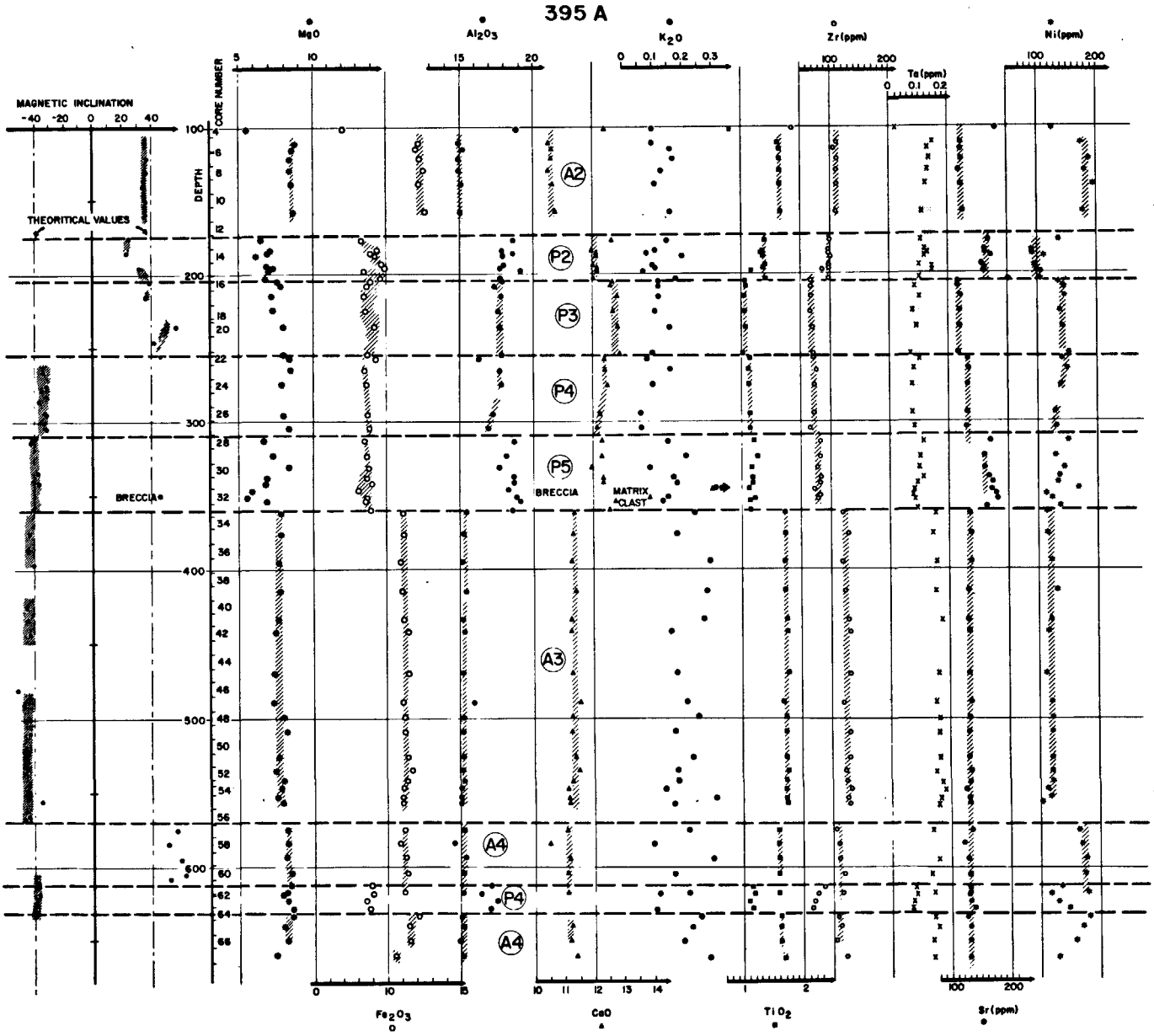

Figure 1. *Selected major and trace elements concentrations versus depth: definition of chemical units.*

TABLE 7
Site 395, Trace-Element Average Values for Each Unit (expressed in ppm)

Unit		A2*	A2*	A2	A3	A4	A4	A4	P1*	P2*	P2	P3	P4	P4′	P5
Hole		395 11-1, 105-107 cm	395	395A	395A	upper Core 61 395A	lower Core 61 395A	67-2, 54-59 cm	395	395	395A	395A	395A		
Sc	NA	38.4	37.8	36.6	38.7	36.8	36.8	37.8	30.6	30.6	32.6	31.5	32.1	31.7	30.12
			1.4	1.2	0.7	0.4	0.4				0.4	0.9	0.9	1.5	0.8
Ti	FX	10200	9710	9820	10337	9528	9800	10140	6090	7680	8177	6300	6694	6750	7045
			59	62	152	26	34				137	114	129	216	245
V	FX	301	268	270	306	281	273	297	212	219	235	221	226	229	206
			3.7	2.3	3.6	5.8	5				4	1.7	6.3	18	8
Cr	FX	279	271	270	251	303	296	263	350	222	232	351	– see text –		295
			5	4	6	8	2				4	8			8
Co	FX	48	48.6	49.5	42.7	46.8	46.3	44	37.5	34	37.6	38.8	39.4	38.5	37
			1	8	1.5	1.3	1.1				1.5	.7	1.4	.6	1.1
Co	NA	49	49.7	49.6	43.4	47.3	47.3	44	39.5	35	38.1	40.5	40.8	40.2	38.2
			0.5	0.5	0.7	0.6	0.6				0.7	1.4	1.6	1.5	1.
Ni	FX	161	176	178	117	172	169	129	135	86	94.8	140			136.1
			3.9	4.8	4.4	6.5	11				8	4.6	– see text –		7.6
Ni	NA	160	185	182	118	176	176	131	145	90	101	143.6			145.3
			3.3	9.5	3.8	5.5	5				4.6	8.2			11
Cu	AA	69	67.8	72.8	57.8	65.5	60.3	54	64	55	60.6	65.8	69	64.7	59.5
			2	2.3	2.1	3.5	2.9				1.3	3.2	2.9	4.3	2.5
Zn	AA	92	85.5	84.2	84.6	81.5	84.5	83	55	58	64.3	59	63.8	65	64
			2.8	2.1	5.6	1.9	2.4				2.5	3.7	3.3	2.6	3.3
Sr	FX	127	119	121	131.2	127.5	129	132	113	162	162	117	135.6	132.2	163.8
			1	2.4	2	6.5	2.4				5	2.8	2.1	4.7	5.6
Zr	FX	121	116	110	125.6	111.2	109	124	67	94	97.6	67	72.1	73.5	78.2
			3.3	2.3	4.8	5.6	4.1				1.6	2.2	4.9	9	5
Zr	NA	112	118	115	131.8	114.7	116	112	65	98	104.8	73	82.3	74.2	88.6
			11	15	8.7	4.2	10				12	6.2	7.1	7.6	7.2
La	NA	3.25	3.39	3.25	4.1	3.5	3.6	4.0	2.0	2.8	3.0	2.1	2.2	2.2	2.45
			0.3	0.1	0.1	0.1	0.1				0.1	0.1	0.1	0.1	0.2
Eu	NA	1.5	1.39	1.39	1.52	1.41	1.4	1.46	0.96	1.18	1.24	0.97	1.02	1.03	1.07
			0.04	0.07	0.04	0.03	0.03				0.03	0.04	0.03	0.07	0.04
Tb	NA	0.87	0.83	0.82	0.89	0.81	0.82	0.87	0.53	0.64	0.68	0.55	0.56	0.57	0.58
			0.01	0.06	0.03	0.01	0.01		0.01		0.02	0.02	0.01	0.04	0.03
Hf	NA	2.84	2.82	2.79	3.16	2.8	2.93	3.07	1.65	2.21	2.37	1.73	1.88	1.83	1.97
			0.06	0.15	0.09	0.04	0.12				0.09	0.06	0.08	0.14	0.10
Ta	NA	0.2	0.190	0.189	0.228	0.193	0.198	0.225	0.106	0.149	0.161	0.112	0.110	0.106	0.125
			0.004	0.008	0.007	0.002	0.002				0.005	0.004	0.004	0.006	0.007
Th	NA	0.137	0.134	0.130	0.164	0.144	0.147	0.142	0.081	0.113	0.120	0.084	0.083	0.074	0.096
			0.004	0.013	0.017	0.014	0.010				0.012	0.013	0.014	0.009	0.013

TABLE 8
Site 395, Major-Element Average Values for Each Unit (volatile-free concentrations, wt. %)

Unit	A2*	A2*	A2	A3	A4	A4	A4	P1*	P2*	P2	P3	P4	P4′	P5
Hole	395 11-1, 105-107 cm	395	395 A	395 A	395 A upper Core 61	395 A lower Core 61	395 A 67-2, 54-59 cm	395	395	395 A	395 A	395 A	395 A	395 A
No. Samples	1	6	6	16	4	4	1	2	1	8	6	6	4	6
SiO_2	48.9	49.37	49.45	49.73	49.37	48.90	49.90	49.40	49.60	49.71	49.47	49.82	49.47	49.54
		0.32	0.23	0.14	0.77	0.29				0.46	0.37	0.26	0.13	0.35
Al_2O_3	15.93	14.93	15.01	15.14	15.00	15.17	15.10	17.77	18.77	18.04	17.69	17.15	16.90	18.29
		0.12	0.14	0.22	0.36	0.10		0.63		0.32	0.19	0.61	0.47	0.39
Fe_2O_3 (t)	12.83	12.06	12.31	11.20	11.17	11.46	10.56	8.49	9.52	9.33	8.77	8.82	8.87	8.73
		0.15	0.23	0.19	0.23	0.23		0.18		0.49	0.26	0.30	0.20	0.13
MnO	0.20	0.18	0.18	0.18	0.18	0.20	0.17	0.14	0.13	0.14	0.14	0.14	0.14	0.14
		0.01	0.01	0.01	0.01	0.01		0.01		0.01	0.01	0.01	0.01	0.01
MgO	6.8	8.58	8.53	7.61	8.20	8.40	7.30	8.20	6.10	6.84	7.63	7.78	8.35	7.24
		0.20	0.15	0.25	0.14	0.18		0.42		0.41	0.35	0.83	0.19	0.66
CaO	11.01	10.53	10.60	11.29	10.97	11.09	11.40	12.71	12.05	12.13	12.75	12.25	12.03	12.26
		0.03	0.09	0.11	0.32	0.16		0.19		0.21	0.13	0.19	0.10	0.22
Na_2O	2.68	2.66	2.64	2.46	2.40	2.5	2.5	2.15	2.59	2.59	2.16	2.29	2.22	2.48
		0.02	0.04	0.06	0.04					0.08	0.05	0.09	0.01	0.06
K_2O	0.22	0.11	0.14	0.21	0.20	0.23	0.29	0.10	0.30	0.13	0.12	0.14	0.09	0.16
		0.02	0.03	0.05	0.08	0.02		0.04		0.04	0.02	0.05	0.03	0.04
TiO_2	1.70	1.62	1.64	1.72	1.59	1.62	1.69	1.01	1.28	1.37	1.05	1.12	1.13	1.18
		0.01	0.01	0.02	0.01	0.02		0.01		0.03	0.02	0.01	0.04	0.05
P_2O_5	0.18	0.15	0.17	0.17	0.14	0.15	0.15	0.11	0.13	0.14	0.11	0.11	0.10	0.11
		0.01	0.01	0.01	0.01	0.01				0.01	0.01	0.01	0.01	0.02
Total	100.45	100.01	100.67	99.71	99.22	99.72	99.06	100.08	100.47	100.42	99.89	99.62	99.30	100.13
LoI		-0.93	-0.98	-1.34	-1.9	-2.87	-2.60	-1.0	-1.5	-1.84	-1.2	-1.3	-1.85	-1.88

TABLE 9
Site 396, Major-Element Average Values for Each Unit (volatile-free concentrations, wt. %)

	Unit		
	P_a	P_b	P_c
No. Samples	1	4	4
SiO_2	49.3	49.68	49.45
		0.13	0.35
Al_2O_3	16.25	16.78	16.73
		0.10	0.15
Fe_2O_3 (t)	9.96	9.33	9.48
		0.24	0.16
FeO	5.36		
MnO	0.16	0.16	0.16
MgO	7.0	8.17	7.55
		0.31	0.26
CaO	11.57	11.98	12.03
		0.09	0.07
Na_2O	2.40	2.41	2.46
		0.07	0.03
K_2O	0.31	0.24	0.21
		0.04	0.05
TiO_2	1.50	1.27	1.29
		0.02	
P_2O_5	0.15	0.12	0.11
		0.01	0.01
Total	98.60	100.14	99.47
LoI	-2.0	-2.8	2.25
		0.3	0.21

Note: Averages and standard deviations listed for Units P_b and P_c

TABLE 10
Site 396, Trace-Element Average Values for Each Unit (expressed in ppm)

396		Unit		
		P_a	P_b	P_c
No. Samples		1	4	4
Sc	NA	36.8	35	34.7
Ti	FX	9000	7600	7740
V	FX	312	264	255
Cr	FX	288	393	290
Co	FX	40	40	40.5
Co	NA	40.7	41	42
Ni	FX	111	142	121
Ni	NA	114	143	124
Cu	AA	58	66	65
Zn	AA	73	66	72
Sr	FX	148	156	131
Zr	FX	109	87	86
Zr	NA	118	87	97
La	NA	3.5	2.9	2.7
Eu	NA	1.36	1.2	1.22
Tb	NA	.79	0.65	0.68
Hf	NA	2.64	2.2	2.2
Ta	NA	0.21	0.17	0.156
Th	NA	0.16	0.13	0.114

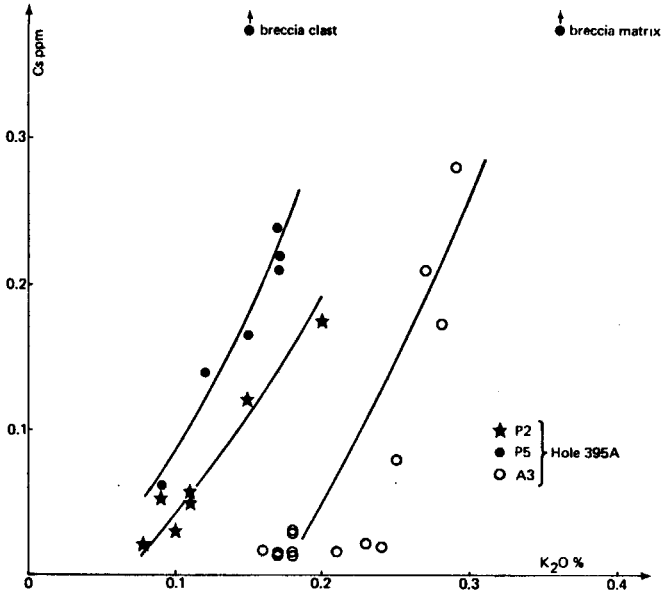

Figure 2. *Cesium versus K_2O; Units P_2, P_5, and A_3 of Hole 395A.*

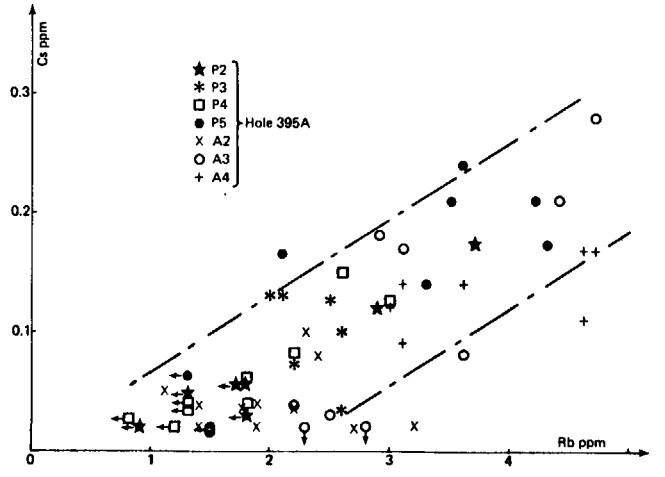

Figure 3. *Cesium versus rubidium; all units of Hole 395A.*

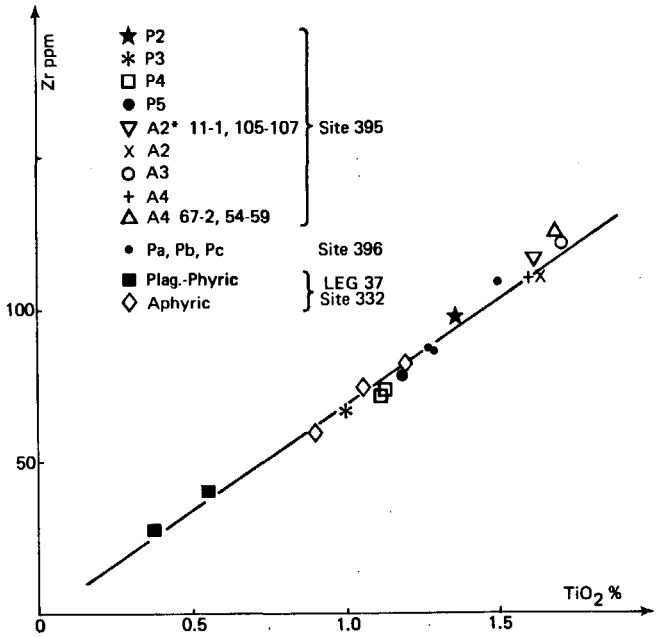

Figure 4. *Zirconium versus titanium (TiO_2); comparisons between Leg 45 and Leg 37 results. Shifts along the line from Leg 37 to Leg 45 samples for phyric samples on one hand and for aphyric samples on the other.*

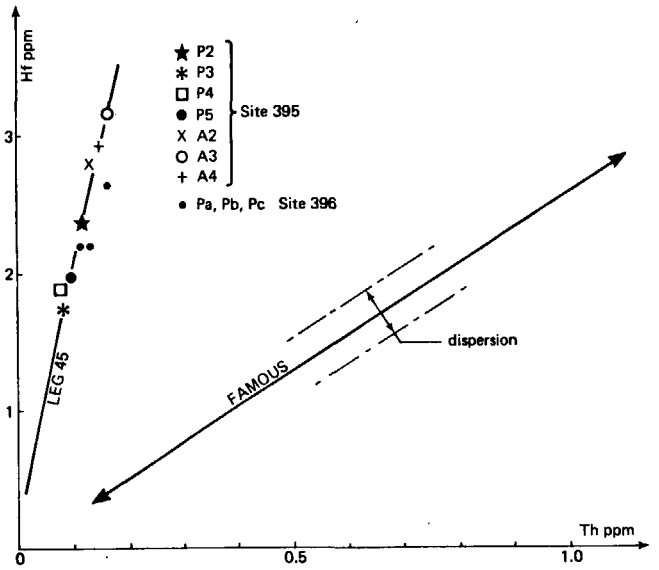

Figure 6. *Hf versus thorium; an LPC element as a function of another very low LPC element, illustrating upper mantle heterogeneity plus variable partial melting (see text).*

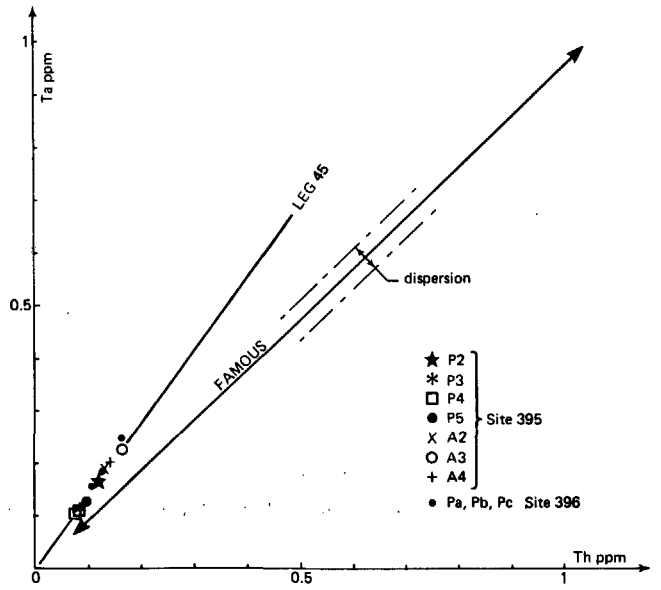

Figure 5. *Tantalum versus thorium; a very low partition coefficient (LPC) hygromagmatophile element as a function of another very low LPC, hygromagmatophile element; upper mantle heterogeneity (see text).*

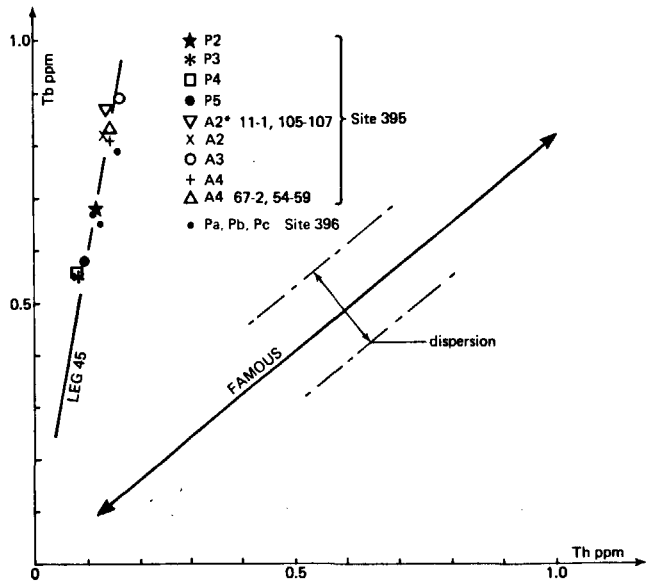

Figure 7. *Terbium versus thorium; an LPC element as a function of another very low LPC element, illustrating mantle heterogeneity plus variable partial melting (see text).*

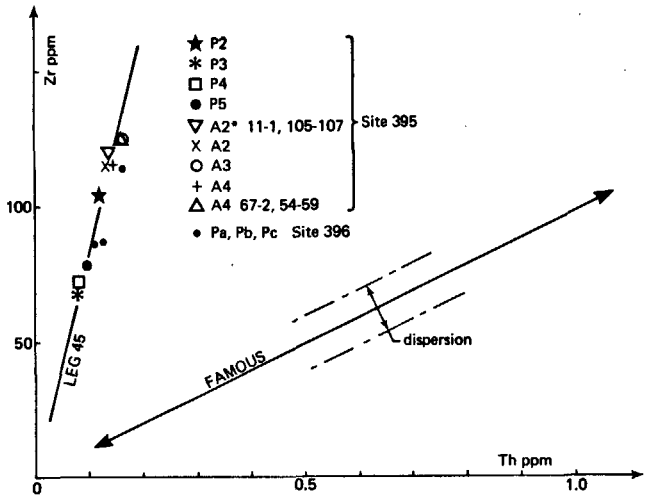

Figure 8. *Zirconium versus thorium; an LPC element as a function of another very low LPC element, illustrating mantle heterogeneity plus variable partial melting (see text).*

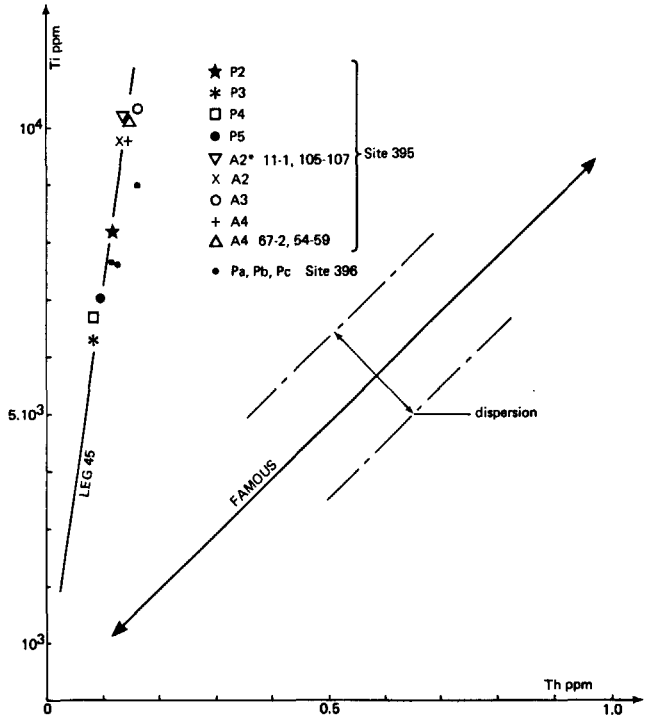

Figure 9. *Titanium versus thorium; an LPC element as a function of another very low LPC element, illustrating mantle heterogeneity plus variable partial melting (see text).*

TABLE 11A
Slope Values of Lines Corresponding to Element i Plotted Versus Element j

j		i = Th	Ta	Hf	Tb	Zr	Ti
Th	F	1	0.95	2.5	0.83	102	9500
	45	1	1.38	20	5.8	830	70000
Ta	F	1.05	1	2.63	0.87	107	10240
	45	0.725	1	14.5	4.2	602	50750
Hf	F	0.40	0.38	1	0.33	40.8	3900
	45	$5\ 10^{-2}$	$6.9\ 10^{-2}$	1	0.29	41.5	3500
Tb	F	1.20	1.14	3	1	122	11700
	45	0.17	0.23	3.4	1	141	11900
Zr	F	$9.8\ 10^{-3}$	$9.3\ 10^{-3}$	$2.45\ 10^{-2}$	$8.13\ 10^{-3}$	1	95.5
	45	$1.2\ 10^{-3}$	$1.65\ 10^{-3}$	$2.4\ 10^{-2}$	$6.96\ 10^{-3}$	1	84
Ti	F	$1.02\ 10^{-4}$	$9.7\ 10^{-5}$	$2.55\ 10^{-4}$	$8.46\ 10^{-5}$	$1.04\ 10^{-2}$	1
	45	$1.43\ 10^{-5}$	$1.97\ 10^{-5}$	$2.86\ 10^{-4}$	$8.29\ 10^{-5}$	$1.18\ 10^{-2}$	1

Note: The dashed line separates values involving either Th or Ta, or both, from values not involving these elements, but which were calculated relative to them. Leg 45 data indicated by 45, FAMOUS data by F.

TABLE 11B
Examples of Absolute Values of LPC Elements for Aphyric and Phyric Samples[a]

		Th	Ta	Hf	Tb	Zr	Ti
Unit A_3							
ARP 7-7	45	0.164	0.228	3.16	0.89	125	10337
	F	0.86	0.85	2.37	0.71	110	8520
Unit P_2							
ARP 31-36	45	0.120	0.161	2.37	0.68	97	8177
	F	0.32	0.28	0.94	0.29	40	3300

[a]A comparison between Leg 45 (45) and FAMOUS area (F).
Note: The dashed line separates representative aphyric or sparsely phyric samples (A_3 and ARP 7-7) from phyric samples (P_2 and ARP 31-36).

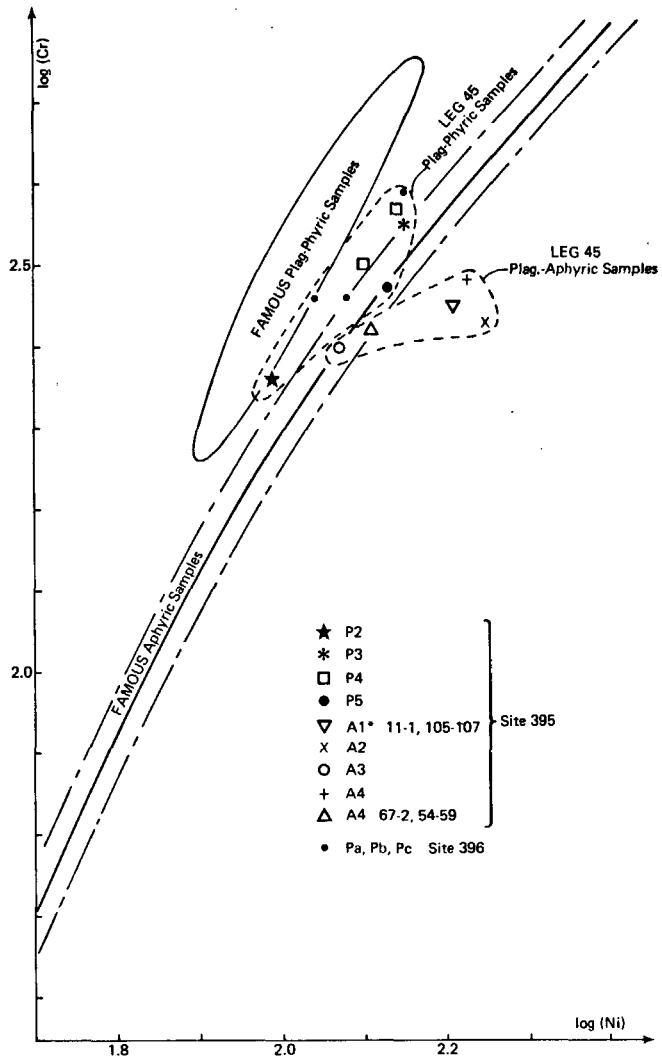

Figure 10. *Log (Cr) versus Log (Ni).*